SUPPORTING MATERIAL

Microsecond unfolding kinetics of sheep prion protein suggests an intermediate that correlates with susceptibility to classical scrapie

Kai-Chun Chen, Ming Xu, William J. Wedemeyer and Heinrich Roder

Table S1: ***Primers for constructing ARR, AHQ, and VRQ variants of ovPrP and the W102F/Y221W mutations***

For A134 → V134 mutation: 5'-GGC TAC ATG CTG GGA AGT GTG ATG AGC AGG CCT CTT ATA C-3' and 5'-GTA TAA GAG GCC TGC TCA TCA CAC TTC CCA GCA TGT AGC C-3'

For R154 → H154 mutation: 5'-GAG GAC CGT TAC TAT CAT GAA AAC ATG TAC CGT TAC CCC-3' and 5'-GGG GTA ACG GTA CAT GTT TTC ATG ATA GTA ACG GTC CTC-3'

For Q171 → R171 mutation: 5'-CTA CAG ACC AGT GGA TCG CTA TAG TAA CCA GAA C-3' and 5'-TTC TGG TTA CTA TAG CGA TCC ACT GGT CTG TAG-3'

For W102 → F102 mutation: 5'-GGT AGC CAC AGT CAG TTC AAC AAG CCC AGT AAG CC-3' and 5'-GGC TTA CTG GGC TTG TTG AAC TGA CTG TGG CTA CC-3'

For Y221 → W221 mutation: 5'-GCA AAT GTG CAT CAC CCA GTG GCA GAG AGA ATC CCA GGC-3' and 5'-GCC TGG GAT TCT CTC TGC CAC ATT TGC-3'

Table S2: χ^2 values indicating the quality of single- vs. double exponential fits to folding/unfolding kinetic traces for the ARQ and ARR variants of ovPrP

ARQ variant

[GuHCl]/M	χ2 (1-exp fit)	χ2 (2-exp fit)
0.85	0.0062	ND
1.19	0.0073	ND
1.55	0.0063	ND
2.04	0.0078	ND
2.23	0.0110	ND
4.00	0.036	0.033
4.43	0.043	0.037
4.81	0.045	0.035
5.21	0.071	0.047
5.62	0.105	0.056
5.96	0.145	0.061

ARR variant

[GuHCl]/M	χ2 (1-exp fit)	χ2 (2-exp fit)
0.84	0.0062	ND
1.19	0.0056	ND
1.51	0.0057	ND
1.85	0.0068	ND
2.01	0.0072	ND
2.35	0.0073	ND
4.0	0.030	ND
4.4	0.030	ND
4.8	0.032	0.029
5.22	0.043	0.035
5.63	0.050	0.037
5.97	0.067	0.042

Figure S1. Calibration of continuous-flow experiments. To determine the dead time and assess the accuracy of continuous-flow mixing experiments, we observed the reaction of with N-acetyltryptophan (NAT) with N-bromosuccinimide (NBS) under pseudo first-order conditions (final concentrations were 10 μM for NAT and 3.3-13.3 mM for NBS). Because NBS is unstable in concentrated solutions of GuHCL and urea, the dead time measurements were carried out in the presence of glycerol to match the viscosity of the GuHCl denaturant under the initial and final conditions of typical refolding (panel **A**) and unfolding experiments (panel **B**). For these tests, we chose NAT rather than the conventional N-acetyltryptophan amide (NATA) because recent results (M. Xu and H. Roder, unpublished) showed that NBS reacts not only with the indole ring, but also with the C-terminal amide protecting group of NATA, giving rise to a second phase with a faster rate constant (10,000 – 30,000 s^{-1}) than oxidation of the indole ring (~30% of the total fluorescence amplitude). In contrast, the NBS oxidation reaction of NAT is very accurately described by a single exponential function (see residual; reduced χ^2 values range from $6x10^{-4}$ to $2x10^{-3}$). In panel A, the initial and final viscosities of a refolding experiment starting at 5 M and ending at 2 M GuHCl were simulated by mixing NAT (53 μM) in 1.15 M glycerol with buffer (50 mM sodium phosphate, pH 7) containing 0.39 M glycerol. In panel B, a typical unfolding experiment (a jump from 2 M to 5.6 M GuHCl) was mimicked by mixing NAT in 0.39 M glycerol with NBS in 1.51 M glycerol. All experiments were done at room temperature, using a flow rate of 1.4 ml/s. Reference traces were obtained by mixing NAT with buffer under matching conditions (fl = 1). The time interval between y-intercept of the single-exponential fits (solid lines) and the first usable point of the kinetic trace is interpreted as the mixing dead time. Dead times ranged from 37 to 43 μs, increasing only slightly with increasing viscosity of the final solution mixture.

Fig. S1 A: NAT-NBS dead-time calibration under refolding conditions

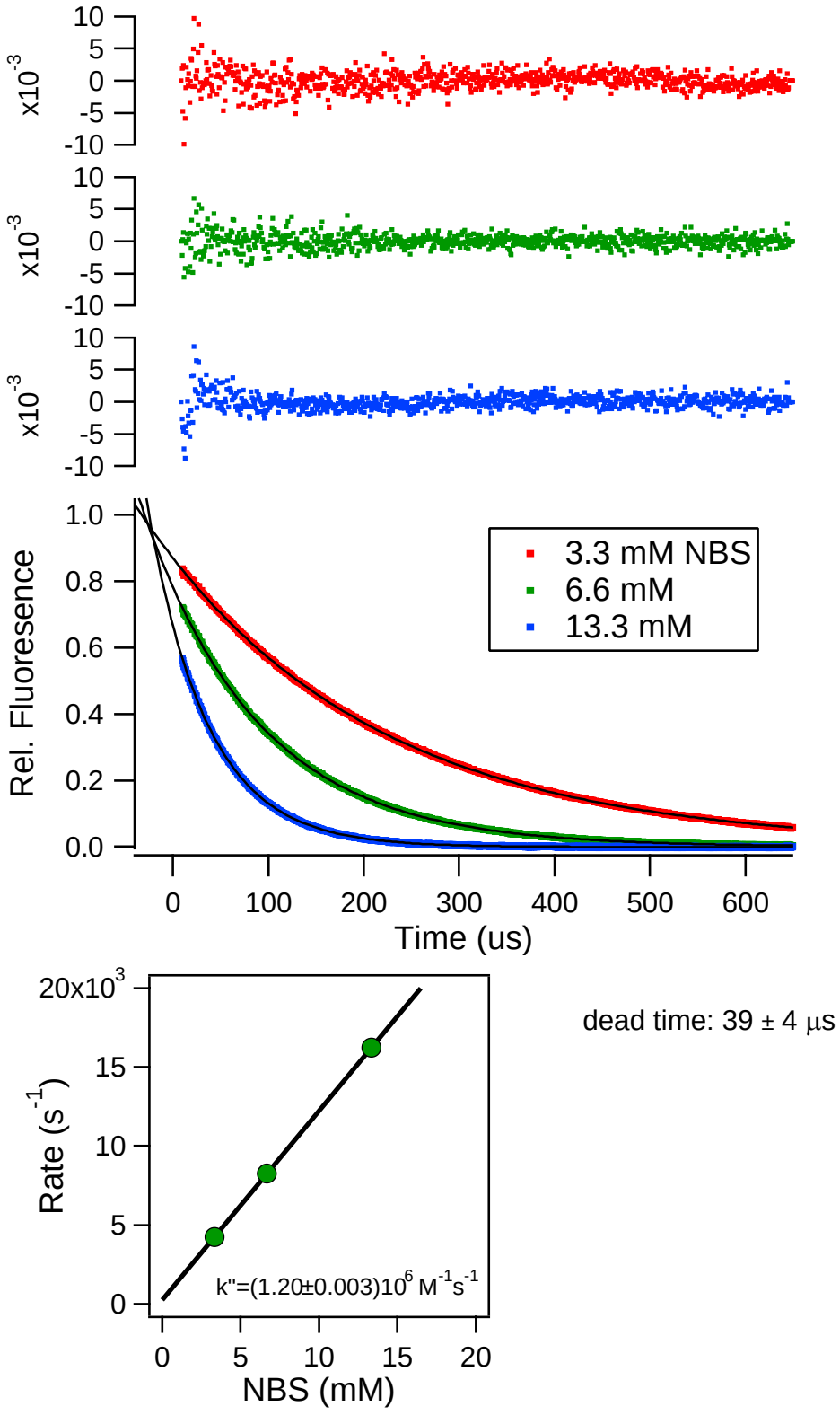

Fig. S1 B: NAT-NBS dead-time calibration under unfolding conditions

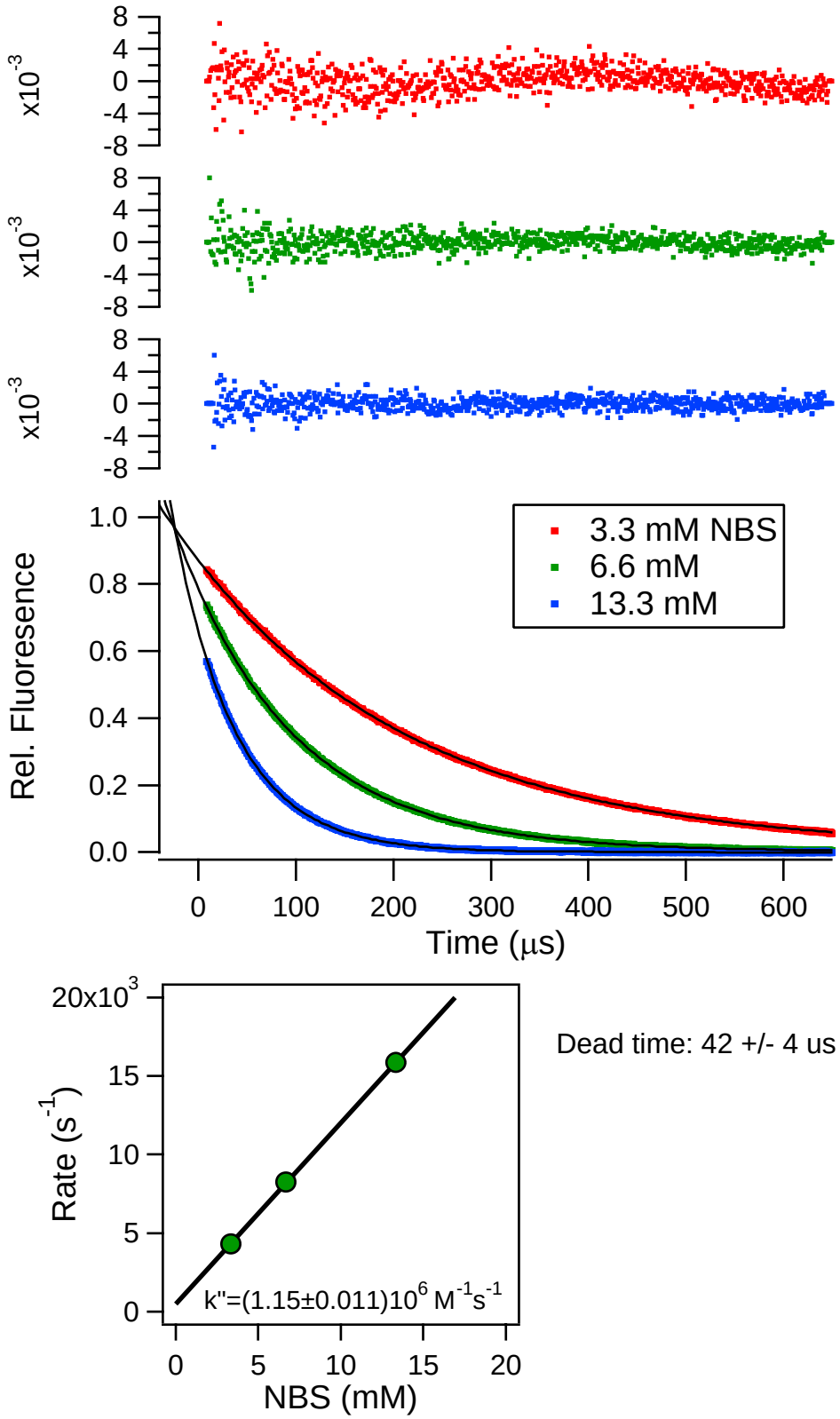

Figure S2. Concentration profile of sedimentation equilibrium. The concentration profile assumes a Boltzmann distribution, indicating that ovPrP is monomeric. Measurements were carried out in 50 mM sodium acetate, pH 5.

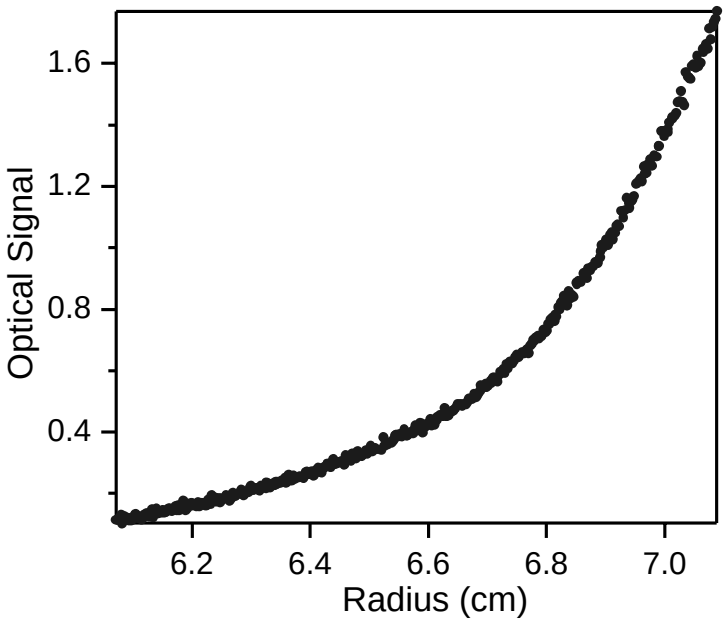

Figure S3. Representative kinetic trace observed in ovPrP refolding experiments. This refolding kinetic trace of the ARQ variant (red dots) was taken in the presence of 1.45 M GuHCl at pH 5 and 15^{o}C with the best fit to one exponential (solid line). Residuals of the fit are shown in the upper panel Refolding data was normalized by the fluorescence signal of unfolded ovPrP. As shown in the figure, one exponential suffices to fit the data accurately. Similar fitting situation was encountered for refolding traces of all the ovPrP variants taken in different solution conditions.

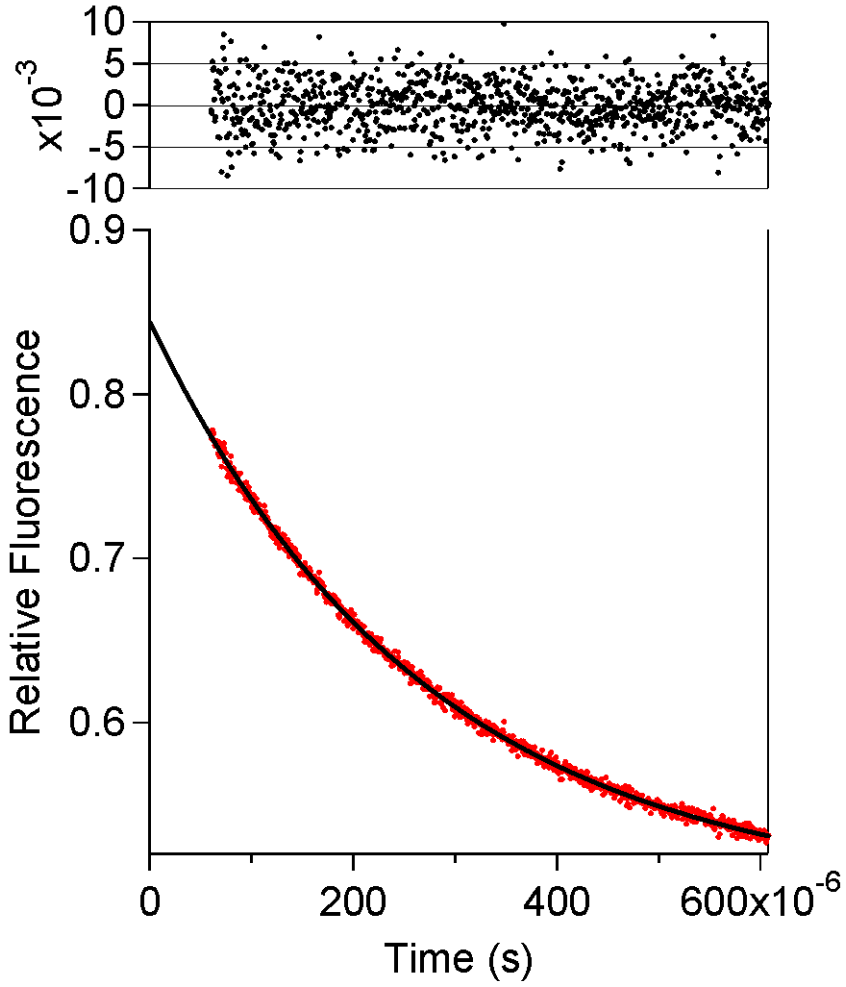

Figure S4. Refolding kinetic traces for ovPrPs in the presence of various concentrations of GuHCl at either pH 5 (A-D) or pH 7 (E-F), 15°C. The fluorescence signal was normalized by the fluorescence of unfolded ovPrP. Solid lines represent single-exponential fits to the kinetic traces.

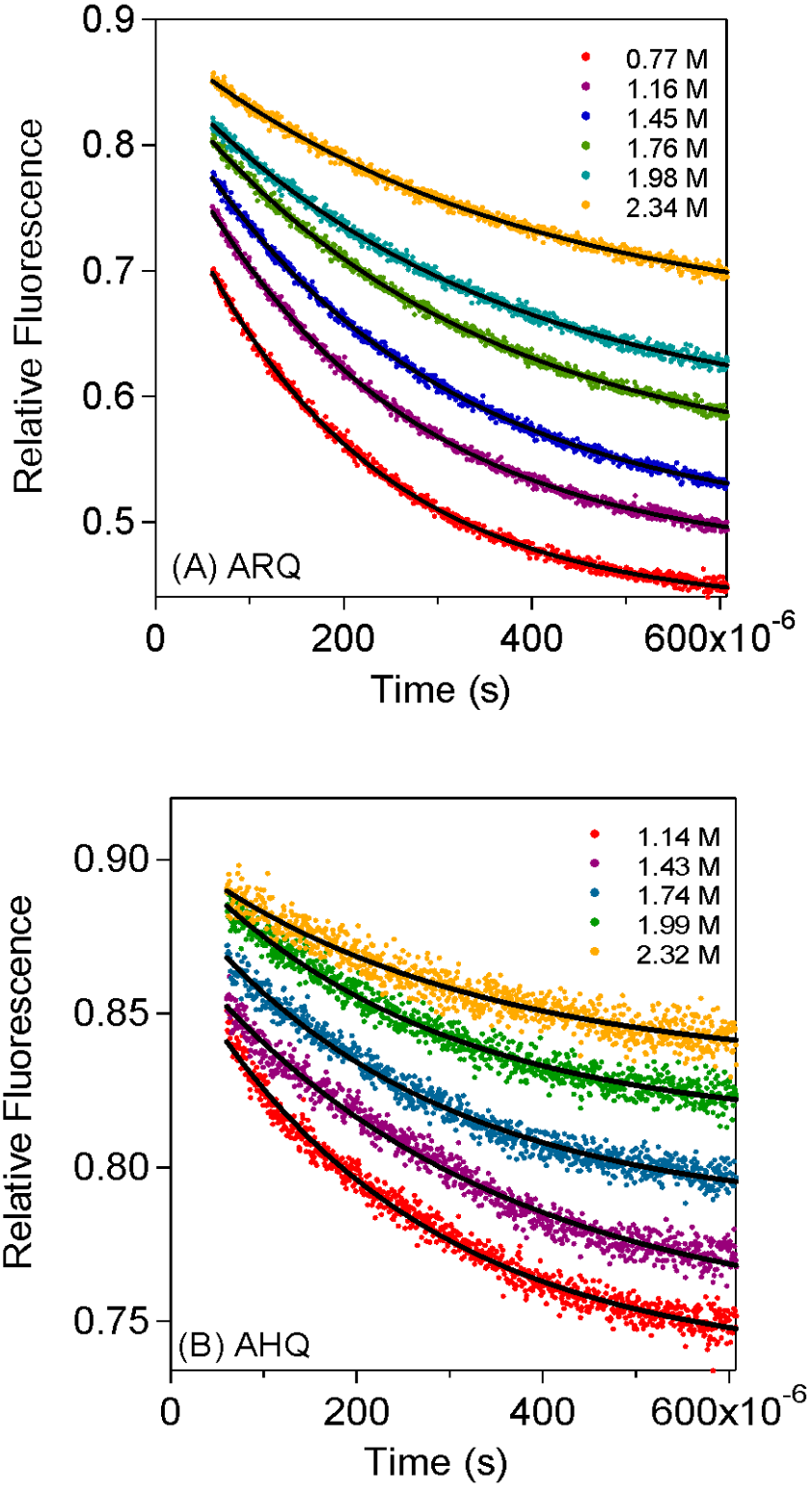

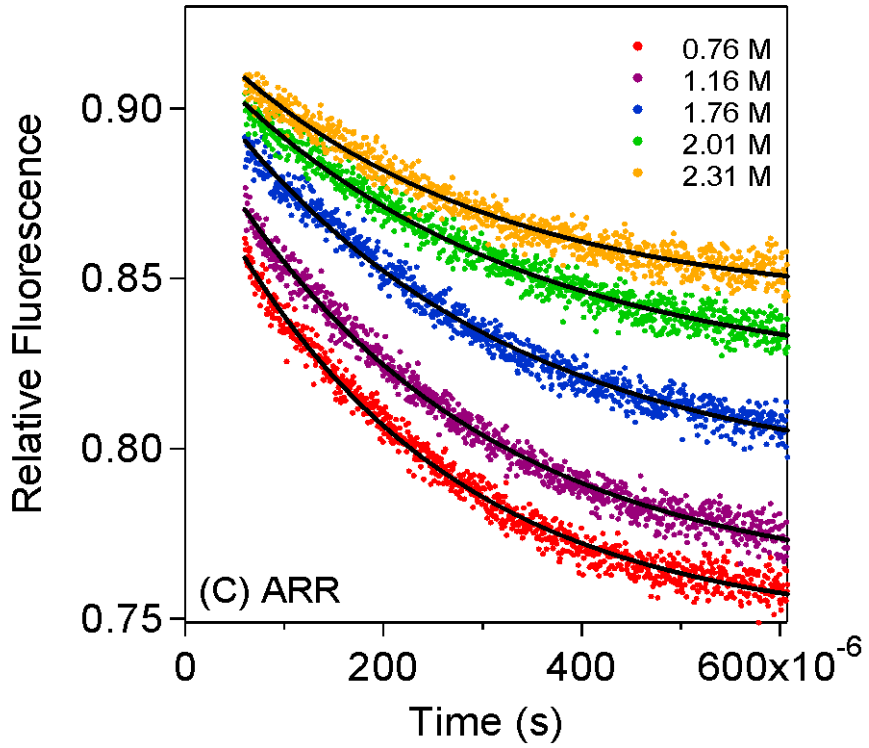
0.76 M
1.16 M
1.76 M
2.01 M
2.31 M
(C) ARR
Relative Fluorescence
0.90
0.85
0.80
0.75
0
200
400
600x10-6
Time (s)

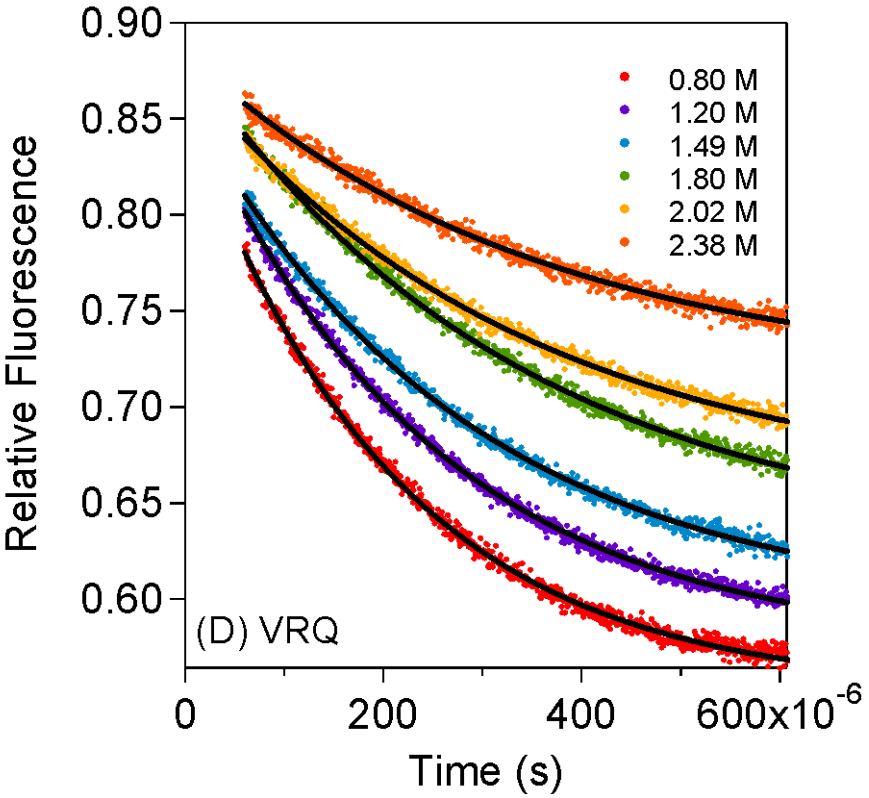
0.80 M
1.20 M
1.49 M
1.80 M
2.02 M
2.38 M
(D) VRQ
Relative Fluorescence
0.90
0.85
0.80
0.75
0.70
0.65
0.60
0
200
400
600x10-6
Time (s)

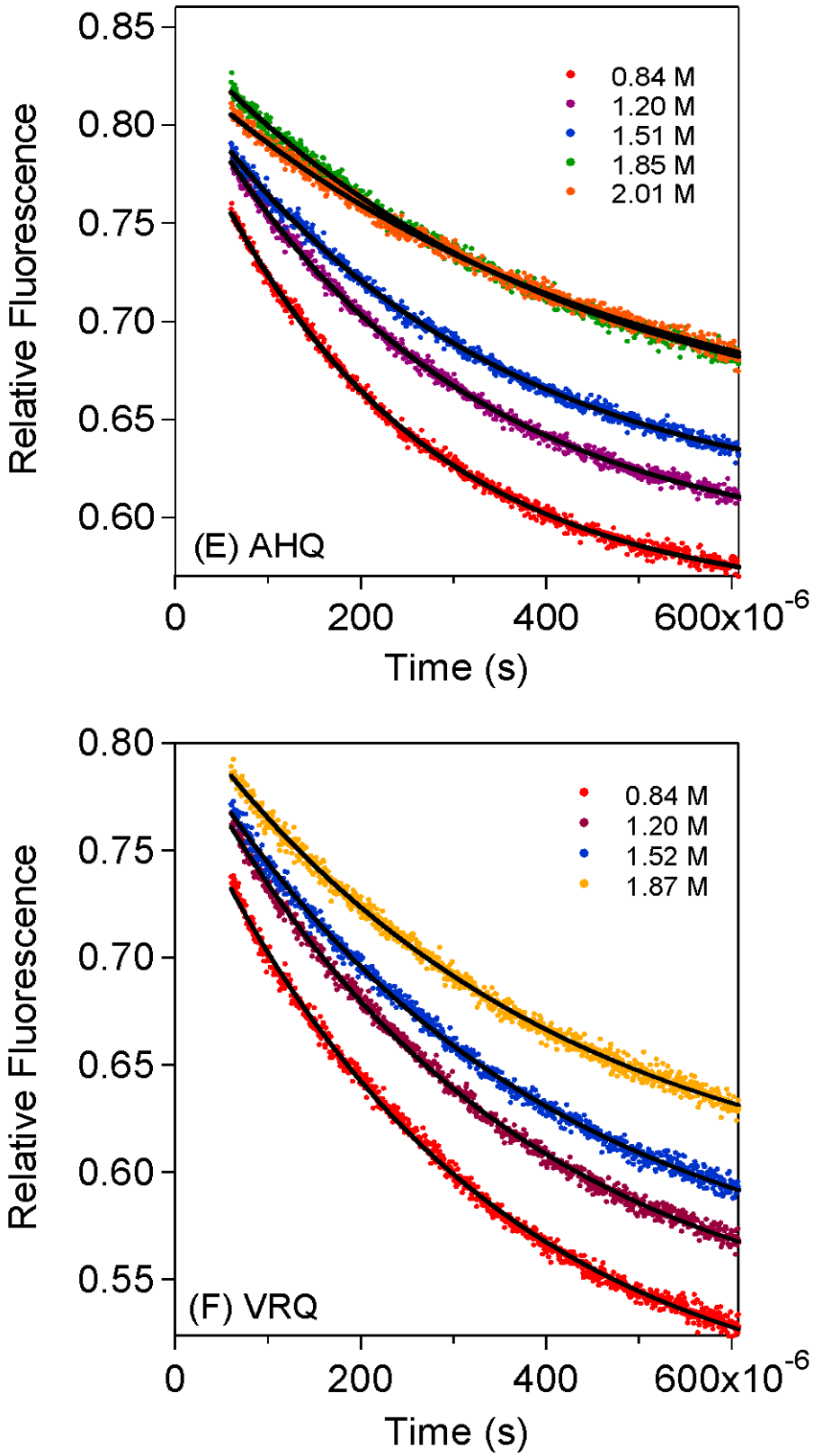
0.85
0.80
0.75
0.70
0.65
0.60
Relative Fluorescence
0.84 M
1.20 M
1.51 M
1.85 M
2.01 M
(E) AHQ
0
200
400
600x10-6
Time (s)
0.80
0.75
0.70
0.65
0.60
0.55
Relative Fluorescence
0.84 M
1.20 M
1.52 M
1.87 M
(F) VRQ
0
200
400
600x10-6
Time (s)

Figure S5. Refolding kinetic traces for ovPrPs in the presence of various concentrations of urea or GuHCl. Continuous-flow experiments in (A): GuHCl at pH 7, 5^{o}C, (B): urea at pH 5, 15^{o}C, (C): urea at pH 7, 5^{o}C. The fluorescence signal was normalized by the fluorescence of unfolded ovPrP. Solid lines represent one-exponential fits to the kinetic traces.

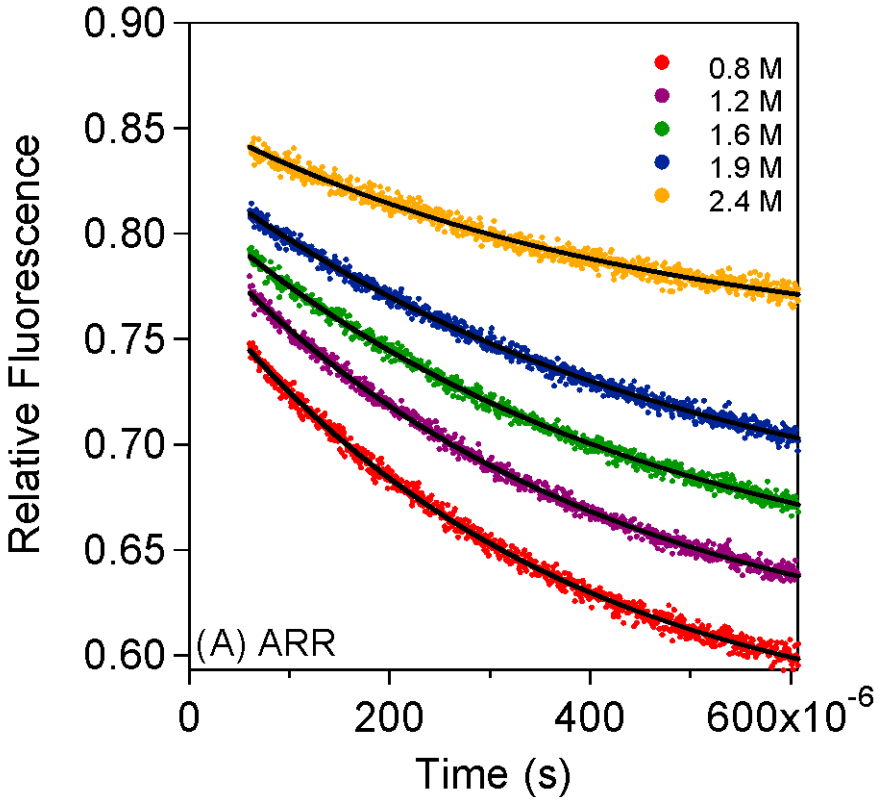

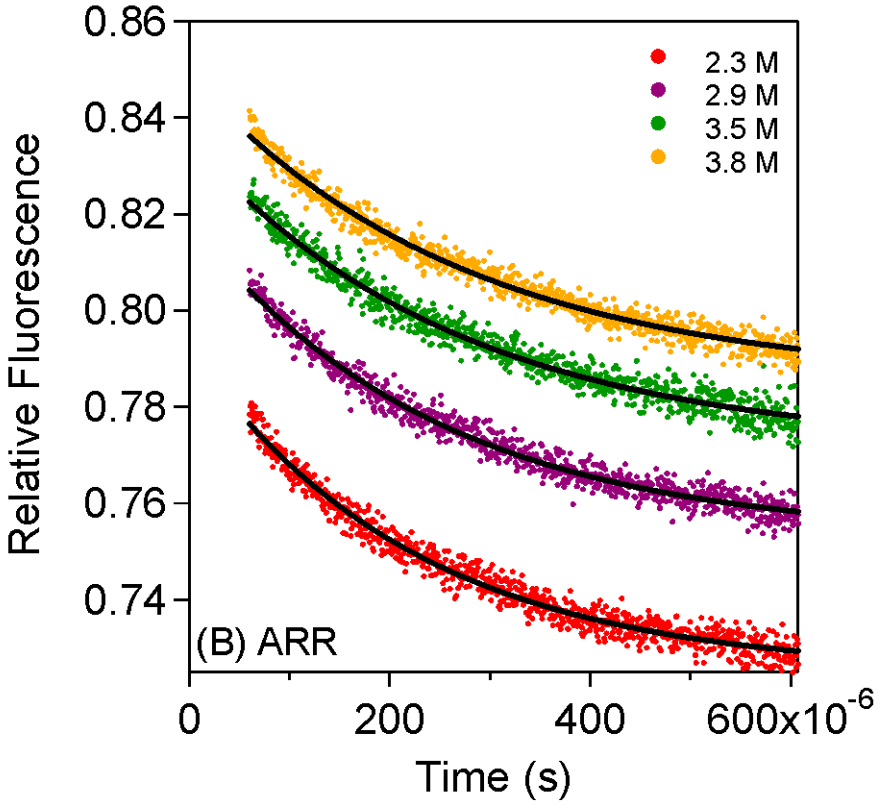
0.86
0.84
0.82
0.80
0.78
0.76
0.74
Relative Fluorescence
2.3 M
2.9 M
3.5 M
3.8 M
(B) ARR
0
200
400
600x10-6
Time (s)

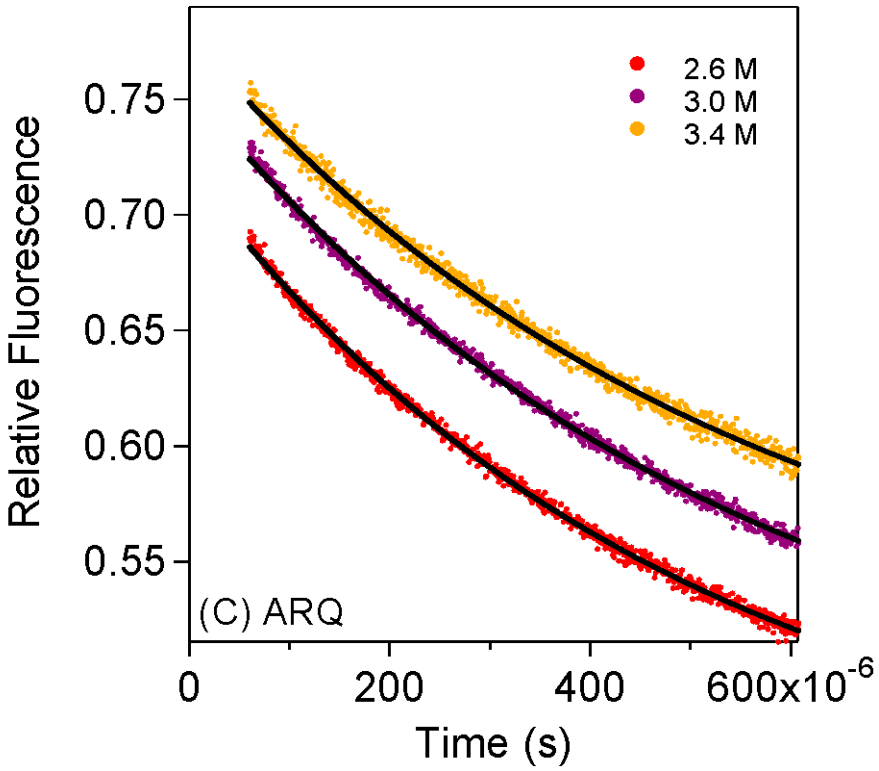
0.75
0.70
0.65
0.60
0.55
Relative Fluorescence
2.6 M
3.0 M
3.4 M
(C) ARQ
0
200
400
600x10-6
Time (s)

Figure S6. Global modeling of the kinetics of folding/unfolding of ovPrP variants ARQ (left panels) and ARR (right panels). The kinetics of folding (A and B) and unfolding (C and D) was measured in the presence of various concentrations of GuHCl at pH 7, 15^{o}C (see Fig. 2). Solid lines represent the time course of folding (A and B) and unfolding (C and D) predicted by global analysis of the kinetic data for each variant using a sequential three-state mechanism (***U*↔*I*↔*N***).